Holographic recording of unslanted volume transmission gratings in Acrylamide/Propargyl acrylate hydrogel layers: towards nucleic acids biosensing.

Paola Zezza , María Isabel Lucío , Izabela Naydenova , María-José Bañuls * , Ángel Maquieira

Posted Date: 31 July 2023

doi: 10.20944/preprints202307.2074.v1

Keywords: Holographic recording; volume transmission grating; hydrogel layer; diffraction efficiency; biosensor.

Article

Holographic Recording of Unslanted Volume Transmission Gratings in Acrylamide/Propargyl Acrylate Hydrogel Layers: Towards Nucleic Acids Biosensing

Paola Zezza [1,3,4], María Isabel Lucío [1], Izabela Naydenova [3,4], María-José Bañuls [1,2,*] and Ángel Maquieira [1,2]

[1] Instituto Interuniversitario de Investigación de Reconocimiento Molecular y Desarrollo Tecnológico (IDM), Universitat Politécnica de Valéncia, Universitat de Valéncia, Camino de Vera s/n, 46022, Valencia, Spain
[2] Departamento de Quimica, Universitat Politécnica de Valéncia, Camino de Vera s/n, 46022, Valencia, Spain
[3] School of Physics and Clinical and Optometric Sciences, Technological University Dublin, City Center Campus, Dublin, Ireland
[4] Centre for Industrial and Engineering Optics, Technological University Dublin, City Center Campus, Dublin, Ireland.
* Correspondence: author: mbpolo@upv.es

Abstract: The role of volume hydrogel holographic gratings as optical transducers in sensor devices for point-of-care applications is increasing due to their ability to be functionalized for achieving enhanced selectivity. The first step in the development of these transducers is the optimization of the holographic recording process. The optimization aims at achieving gratings with reproducible diffraction efficiency, which remains stable after reiterative washings, typically required when working with analytes of biological nature or several step tests. The recording process of volume phase transmission gratings within acrylamide/propargyl acrylate hydrogel layers reported in this work was successfully performed and the obtained diffraction gratings were optically characterized. Unslanted volume transmission gratings were recorded in the hydrogel layers and using the optimized conditions, diffraction efficiencies of up to 80% were achieved. Additionally, the recorded gratings demonstrated to be stable in water after multiple washings. The hydrogels, after functionalization with oligonucleotide probes yields specific hybridization response, recognizing the complementary strand as demonstrated by fluorescence. Analyte-sensitive hydrogel layers with holographic structures are a promising candidate for the next generation of *in vitro* diagnostic tests.

Keywords: holographic recording; volume transmission grating; hydrogel layer; diffraction efficiency; biosensor

1. Introduction

Holographic biosensors are emerging as a new technology for the development of portable analytical devices for label-free detection applications [1]. Holograms offer a direct transduction method with several advantages such as fast response, and high sensitivity. Typically, holograms are recorded in various photosensitive materials, such as silver halide films, dichromated gelatins or photopolymers [2]. Self-processing materials such as photopolymers are the most used in recent years, since they have excellent holographic characteristics and low cost [3]. Recently, hydrogels have attracted attention for holographic sensing applications [4]. These materials are made of three-dimensional polymeric networks of hydrophilic polymers with a high water-absorbing capacity [5]. Moreover, their composition can be fine-tuned in order to obtain appropriate chemical, mechanical and biological characteristics, enabling the incorporation of specific probes such as oligonucleotides, proteins and others [6]. Hydrogels as support matrices for biosensing allow high incorporation of

 doi:10.20944/preprints202307.2074.v1

recognition elements in three dimensions and provide an aqueous and biocompatible microenvironment. For the fabrication of holographic gratings in hydrogels, it is important to obtain a transparent layer with good optical quality and high permeability. Holographic recording in light-sensitive materials is based on the process of photoinduced polymerization [7]. The fabrication method of volume holographic gratings consists of impregnating the recording layer with a light-absorbing material and exposing it to laser light with periodically varying intensity. Normally, a mixture of monomers, a crosslinker, a free radical generator and a dye photosensitizer are required for the recording of volume transmission gratings [8]. Photopolymers usually contain a polymeric binder in addition to the other components, which allows for dry layers [9], but the use of hydrogels as holographic matrices is strongly appealing for obtaining materials stable in aqueous environment [10,11]. On exposure to light, the photosensitizer dye reacts through electron transfer to generate free radicals so that polymerization can begin. Hence, the components of the recording material are spatially redistributed when illuminated by an optical interference pattern, resulting in a holographic volume grating. The formation of the grating involves a spatial variation in the density of the polymeric layer due to diffusion driven by the concentration gradient of monomer molecules, from non-irradiated to irradiated areas. [12]. The overall refractive index is higher in the polymerized region than in the unpolymerized one due to the higher density of polymer when compared to monomer (VTG recording, Figure S1, Supporting info). The achieved diffraction efficiency of the recorded hologram depends on many factors, such as the parameters used during recording, such as exposure time and laser intensity, and, on the other hand, the chemical composition and thickness of the recording layer [13]. Holographic sensor, and biosensors in particular, are still at an early stage of development. In fact, most common applications focus on physical and chemical sensing (humidity, pH, gases and solvents), but not on biosensing [14]. The principle of detection of holographic biosensors is based on the alteration of the diffraction efficiency when interaction with the target biomolecule (e.g., DNA strand) occurs. Alternatively, a change in the period of the recorded grating can occur due to shrinkage or swelling of the material leading to a change in the angular position of the Bragg peak. Light-sensitive hydrogels functionalized with analyte-sensitive units represent an unexplored opportunity for the fabrication of holographic biosensors.

To date, relatively few holographic gratings have been obtained in hydrogels and used as transducers for biosensing. It is of great interest to exploit the potential of this promising sensing technique and make it applicable for monitoring different targets. Notably, the transduction of the detector signal into a simple optical readout by holographic gratings can be useful for point-of-care diagnostic devices. A significant advantage of holographic gratings based on hydrogel biosensors is that they enable the detection of analytes without labelling, thus eliminating the need for additional labels or reagents. Another beneficial aspect of hydrogel-based biosensors is that their composition can be tuned, and they can be easily functionalized with recognition molecules, including enzymes, antibodies, nucleic acids and aptamers, using conventional bio-conjugation techniques. However, there are still some challenges to overcome for the use of this methodology for applications as label-free biosensors. To achieve good analytical performance of holographic hydrogel-based biosensors, the immobilized recognition element plays a crucial role and additional labelling, and signal amplification strategies are often required. Alternatively, the performance of the hydrogel-based holographic grating can be further improved by optimizing the diffractive grating design. Another challenge is to obtain quantitative and repeatable results, due to the difficulty of controlling the quality of the gratings, especially in soft materials such as hydrogels.

Holography- based transduction method has been successfully demonstrated for the detection of biomolecules, volatile organic compounds and metal ions [15]. For example, volume holographic gratings (VHGs) based on hydrogels as sensing platforms have been widely employed for the measure of pH [16], humidity and temperature [17,18], metal ions [19,20], and glucose [21,22]. However, to our knowledge, direct detection of oligonucleotides has not yet been performed by holographic sensing. This means that there are no biosensors based on this technology that can detect DNA or RNA.

 doi:10.20944/preprints202307.2074.v1

This work focused on the optimisation of the recording process of unslanted volume transmission gratings (VTGs) in Acrylamide/Propargyl Acrylate (AM/PA) hydrogel layers. The composition of the hydrogel had already been optimized in previous work in which hydrogels were surface micropatterned and utilized as biosensors [23]. By using this hydrogel composition, the bioreceptor elements (thiol-modified DNA probes) can be covalently immobilized via thiol-yne click reaction both before and after the fabrication of the volume grating. The aim of this work is to record holographic gratings in hydrogel layers with high diffraction efficiencies, for achieving improved sensitivity of the designed holographic biosensor. In fact, phase holograms recorded in the volume of the layer offer the advantage of achieving diffraction efficiency nearly 100%, much higher than surface gratings with diffraction efficiencies around 30% [24]. Herein, unslanted volume transmission gratings (VTGs) were recorded directly in (AM/PA) hydrogel layers, to the best of our knowledge for the first time. Also, their capability to be biofunctionalized with an oligonucleotide probe covalently attached, and to perform specific hybridization keeping their diffractive property is demonstrated. Initially, (AM/PA) hydrogel layers were prepared by thermal activation. Afterwards, to carry out the recording of unslanted VTGs, the hydrogel layers were incubated in dark with the incubation solution. This solution contains an aqueous mixture of acrylamide monomers, N, N-methylene bisacrylamide as crosslinker, triethanolamine (TEA) as initiator and erythrosine B (EB) as dye. To optimize the recording process, different concentrations of the incubation solution and recording parameters were tested. After incubation time, the hydrogels were used in holographic recording, which was observed in real time. At the end of the recording process, the gratings angular Bragg selectivity curves were characterized. Finally, the stability in water of VTGs obtained within hydrogel layers was examined in view of their potential use in biosensing.

2. Materials and Methods

2.1. Materials

Acrylamide (AM), propargyl acrylate (PA), N, N'-methylenebisacrylamide (MBA), potassium persulfate (KPS), triethanolamine (TEA), formamide, 2,2-Dimethoxy-2-phenylacetophenone (DMPA), tris (2-carboxyethyl) phosphine buffer (TCEP), sodium acetate, tetrahydrofuran (THF), sodium chloride, sodium citrate, ethylenediaminetetraacetic acid (EDTA), and erythrosine B (EB) dye were all purchased from Sigma–Aldrich and used without any further purification. The Ac-TCEP buffer, pH 4.5, consists of 25 mM of TCEP, 0.15 M sodium acetate, 0.1 M EDTA, and 0.1 M NaCl in DI water and the saline-sodium citrate buffer (SSC1x, pH 7.4) consists of 0.15 M NaCl and 0.015 M sodium citrate. The oligonucleotides were supplied by Sumilab (Valencia, Spain), and the sequences used are listed in Table S1 (Supporting Information).

2.2. Hydrogel layers preparation

Hydrogel layer preparation was performed using an adapted protocol [11,23]. Briefly, (AM/PA) hydrogels were prepared by mixing 25% (w/v) of AM monomer, 0.05% (w/v) of MBA crosslinker, 75 µL of PA co-monomer and 1% (w/v) of KPS thermal initiator in 5 mL of distilled water. (AM/PA) hydrogel layers were obtained by depositing 500 µL of the pre-polymer solution onto a levelled glass slide (7.5 cm × 2.5 cm) (Labbox Labware, S.L., SLIBG10-050, Premia de Dalt, Spain) provided a mould (5 cm × 1.4 cm × 340 µm). The system was quickly sealed with another glass slide and tightened with two clamps. Hydrogels were synthesized by thermal activation, during 30 minutes at 60 °C (Scheme 1). After the polymerization time, the top glass slide was removed, and hydrogels were soaked overnight in distilled water at RT. The calculated thickness of the hydrogel layer was approximately 300 ± 10 µm.

Preprints (www.preprints.org) | NOT PEER-REVIEWED | Posted: 31 July 2023 doi:10.20944/preprints202307.2074.v1

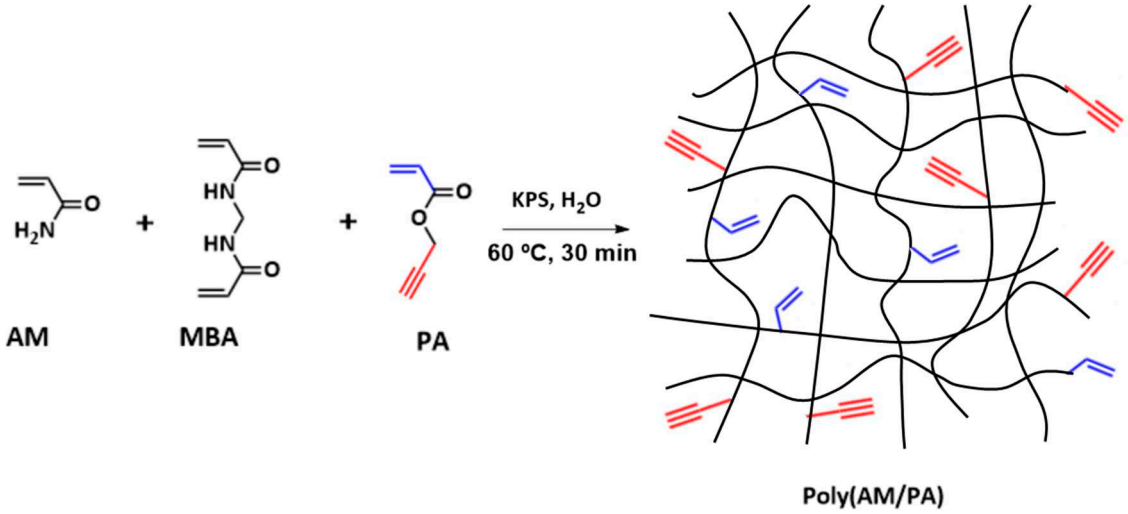

Scheme 1. Representation of the hydrogel synthesis by free-radical polymerization (FRP). AM: Acrylamide, MBA: N, N'-methylenebis (acrylamide), PA: propargyl acrylate, KPS: potassium persulfate. The highlighted functional groups are used for the bioreceptor incorporation. Figure adapted from [23].

2.3. Morphology characterization

The morphological characterization of (AM/PA) hydrogel layers was carried out using scanning electron microscopy (SEM, Gemini SEM 500 system, Zeiss, Oxford Instruments, Oxford, UK). Hydrogels layers were completely swollen in distilled water and frozen at −20 °C. Then, they were lyophilized overnight (Telstar Lyoquest freeze-drier, Azbil Telstar Technologies, S. L. U., Terrasa, Spain) to yield completely dry aerogel samples. Finally, dry samples were prepared using sputter coating with an Au layer of about 15 nm (BAL-TEC SCD 005 sputter coater, Leica microsystems, Wetzlar, Germany).

2.4. Swelling behavior studies

The swelling kinetics were obtained for the (AM/PA) hydrogel. Freeze-dried hydrogel samples of approximately 1 cm^3 were used for this study. The lyophilized samples were immersed in PBS-T (10 mL) at RT and their weight was recorded successively over time until a constant weight (total swelling) was reached. The degree of swelling was calculated using Equation (1), where Wt is the weight of the hydrogel after being immersed in the buffer for a time 't' and W_0 is the weight of the lyophilized hydrogel before buffer immersion.

$$\text{Swelling (\%)} = \frac{Wt - Wo}{Wo} \cdot 100 \quad (1)$$

2.5. Incubation step before recording

Hydrogels layers were prepared for the holographic recording process. Two different incubation solutions were tested (A and B, Table 1). The incubation solutions contained an aqueous mixture of acrylamide, N, N-methylene bisacrylamide as crosslinker, Triethanolamine (TEA) as initiator, and Erythrosine B (EB) as dye. The Erythrosine B (EB) dye was previously dissolved in distilled water at 0.11% (w/v). A volume of 200 µL of incubation solution was deposited on the already polymerized hydrogel layers. The samples then were kept inside a Petri dish in dark at room temperature, until complete absorption of the compounds within the hydrogel matrix was achieved. Different incubation times were tested: 1-day, 2-days and 3-days.

Preprints (www.preprints.org) | NOT PEER-REVIEWED | Posted: 31 July 2023 doi:10.20944/preprints202307.2074.v1

Table 1. Composition of incubation solutions.

Incubation solution	AM (g)	MBA (g)	TEA (mL)	EB (mL)
A	1	0.2	1	4
B	2	0.4	1	4

2.6. Holographic recording and probe set-up

The optical set-up used (Figure 1) consists of a Nd:YVO_4 laser emitting at 532 nm for the recording and a He-Ne laser emitting at 633 nm for the reading (probe laser). Two collimated beams were obtained with equal intensity by splitting the laser light from the Nd:YVO_4 laser with a polarising beam splitter (PBS). The intensity of the two beams was equalized with the help of a half-wave plate (HWP) positioned in front of the PBS, thus allowing for control over the state of polarisation of the linearly polarized beam entering the PBS. After passing through the PBS the beam passed through a second half-waveplate. This was necessary to ensure that both recording beams are with parallel polarisations for achieving maximum visibility of the interference pattern that is being recorded. Both recording beams were s- polarized. The total angle between the two recording beams of 24.6 degree was selected to create an interference pattern of a spatial frequency of 800 lines/mm (the grating period (Λ) was 1.25 μm). To ensure that the recording process was carried out properly, a He-Ne laser beam of 633 nm wavelength was used, as a probe beam, to fully characterise the holograms. The hydrogel samples were placed on a computer-controlled rotational stage (RS) (Newport ESP300). To acquire real-time diffraction efficiency growth (η) and subsequently Bragg selectivity curves, the intensity of the first-order diffracted beam (I_d) was monitored with an optical power meter (Newport Model 840). The signal from the optical power meter was sent to an analogue to digital converter connected to a computer. A LabVIEW programme was used to control the shutters, rotational stage, and the data acquisition. The volume transmission grating spot size was reduced form 1.45 cm^2 to 0.84 cm^2 using a diaphragm.

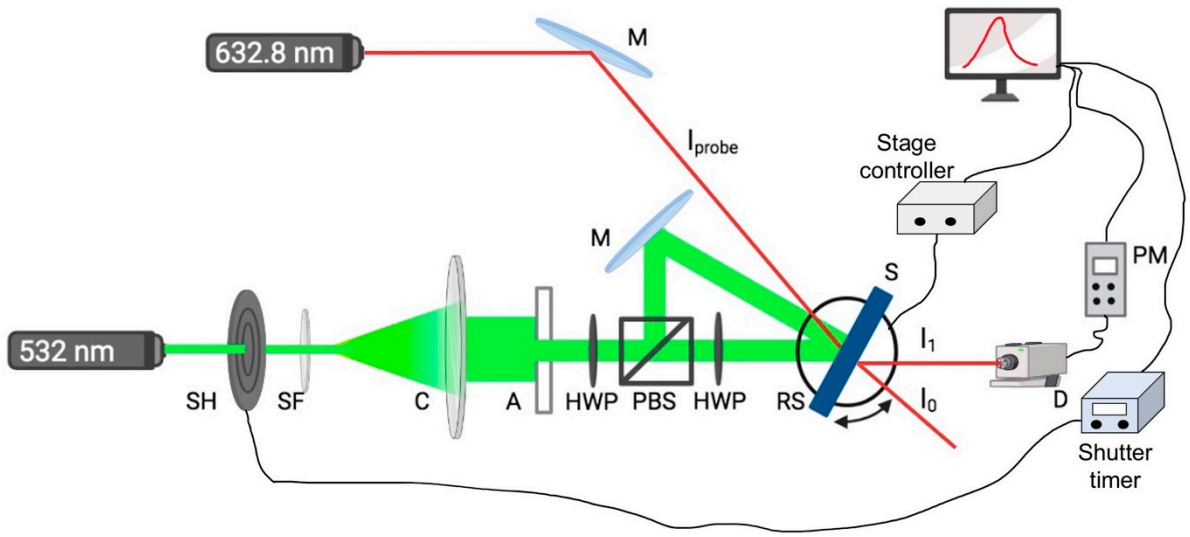

Figure 1. Experimental set-up for the recording of volume transmission gratings. The recording beam wavelength was 523 nm and real-time monitoring was carried out with probe beam of 632.8 nm. Where M: mirror, SH: shutter, SF: spatial filter, C: collimating lens, A: aperture, PBS: beam splitter, HWP: half wave plate; RS: rotational stage, S: sample, D: detector, PM: power meter.

2.7. Holographic recording and characterisation of hydrogel layers

Holographic volume gratings were recorded within hydrogel layers using transmission geometry (Figure S1a). Specifically, phase holograms were recorded through the laser light-induced

photopolymerization process, which leads to the modulation of the refractive index within the hydrogel layer. Volume transmission gratings (VTGs) were recorded directly on Acrylamide/Propargyl acrylate hydrogel layers using the unslanted configuration, in which the two recording beams have equal angles of incidence. Recording parameters such as green laser power and exposure time were optimized for the recording process. Development of the hydrogel holographic gratings was monitored by measuring the diffraction efficiency (DE% or η) growth curves in real-time with the probe beam (red). The diffraction efficiency of the recorded VTGs was calculated as the ratio of the diffracted beam intensity (I_d) and the incident beam intensity (I_{probe}) per cent. To observe the dependence of the intensity of the diffracted light (I_d) on the angle of incidence of the probe beam, Bragg selectivity curves of hydrogel VTGs were obtained by rotating the sample holder placed on a high accuracy rotational stage (model Newport ESP300 with angular resolution of 0.001º). After recording, hydrogels were immersed in distilled water and the diffraction efficiency was measured after several washes, to verify the stability of the recorded VTGs. In addition, Kogelnik's coupled-wave theory was used to fit the Bragg angular selectivity curves of the gratings and thus extract the thickness of the layers and the refractive index modulation created during the recording process [25].

2.8. Biofuncionalization of VTGs and hybridization/dehybridization experiments

For future biosensing applications, the VTG layers were covalently functionalized with a thiol-modified DNA probe via the thiol-ene/thiol-yne coupling photo-click reaction [23]. A 1 mL solution of a 1:1 THF:Ac-TCEP mixture at 5 µM of functionalization probe was prepared and 1% (w/v) DMPA photoinitiator was added. VTG hydrogels were placed inside circular containers with 300 µL of the prepared probe solution and irradiated at 365 nm in a UV photoreactor, LightOx PhotoReact (13 mW/cm^2 light power) (Sigma–Aldrich, Madrid, Spain) for 30 min. Then, biofunctionalized VTGs were washed overnight in SSC1x. DE was monitored before and after the biofunctionalization in SSC1x. Biofunctionalized VTGs were incubated with serial increasing concentrations of Cy5-labeled complementary or non-complementary sequence as a target (0.2; 0.5; 1 and 2 µM) for 1h and washed for 1 h with SSC1x. The fluorescence signal was monitored after every washing step using a homemade surface fluorescence reader (SFR) equipped with a CCD camera [26] (λ=647 nm, exposure time = 10 s, gain = 1). Fluorescence image data processing was performed with the GenePix Pro 4.0 software from Molecular Devices, Inc. (Sunnyvale, CA, USA). The probe and targets used are listed in Table S1 (Supporting Information). Dehybridization of VTGs hybridized with 1 µM of labeled complementary target after their washing with SSC1x was carried out by different approximations: a) immersion of the VTGs in 5 mL of H_2O for 16 h at RT, b) immersion of the VTGs in 5 mL of H_2O for 1 h at 90 °C, and c) immersion in 5 mL SSC1x, 50 % formamide. Fluorescence was registered after every step (λ=647 nm, exposure time= 5 s, gain= 1). A second hybridization step was carried out with the VTGs dehybridized with SSC1x, 50% formamide, with labeled complementary and not-complementary target at 5 µM, following the previously described protocol. Fluorescence was registered after washing with SSC1x (λ=647 nm, exposure time= 5 s, gain= 1)

3. Results and Discussions

Thin films of hydrogels composed of AA, MBA and PA were prepared adapting the described protocol [11,23]. The morphology of the lyophilized (AM/PA) hydrogel was characterized by SEM microscopy (Figure 2a). The typical porous structure of MBA-AA hydrogels of low crosslinking degree can be observed. The swelling of the hydrogel layer is important to ensure that it is sufficiently permeable to facilitate the diffusion of the incubation solution. Figure 2b shows the swelling degree of the lyophilized layers over time. These hydrogels reached approximately 500% of swelling at 24 h which is associated with the porosity of the hydrogel layer. In order to achieve reproducible holographic recording in hydrogel layers, initially two different compositions of the incubation solution and then different recording parameters were tested. (AM/PA) hydrogel layers were placed in Petri dishes in dark at room temperature and wetted with 200 µL of the incubation solution. Thus, components of the incubation solution can penetrate the layer and thus participate in the

Preprints (www.preprints.org) | NOT PEER-REVIEWED | Posted: 31 July 2023 doi:10.20944/preprints202307.2074.v1

photopolymerization. This process leading to holographic recording begins with the absorption of laser light by the sensitising dye (erythrosine B). After absorbing a photon, the sensitiser is promoted to an excited state and reacts with the electron donor (TEA) to produce TEA free radicals. These free radicals react with the monomers to initiate free-radical polymerisation. Therefore, the optical sensitivity of the hydrogel to the wavelength of the recording beam is influenced by the concentration of the components in the incubation solution. The most important aspect observed for holographic recording in hydrogels is that it is essential that the hydrogel layer reaches complete swelling in water prior to the incubation phase. In fact, no effective holographic recording was achieved for non-hydrated (AM/PA) hydrogel layers using these volumes of incubation solution. In contrast, high diffraction efficiencies were obtained for the hydrogel layers after 24 hours of complete swelling in distilled water.

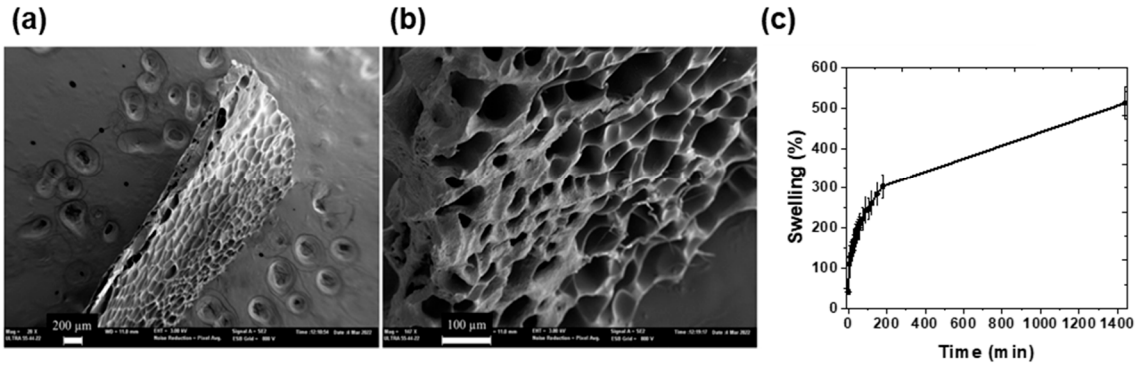

Figure 2. (a) and (b) SEM images of the cross section of the hydrogel films at different magnifications fully hydrated and then lyophilized and (b) Swelling kinetic study of (AM/PA) hydrogel in PBS-T, using synthesised samples with a size of 1 cm^3. .

Two different incubation solutions, A and B (Table 1) were tested for the recording process. For this experiment, incubation was carried out for 1 day. The DE was monitored at the same time that the VTGs were being recorded. Better results were observed with incubation solution A. In the case of solution B, it was observed that the real-time growth curve of the diffraction efficiency initially increases and then suddenly starts decreasing (Figure 3).

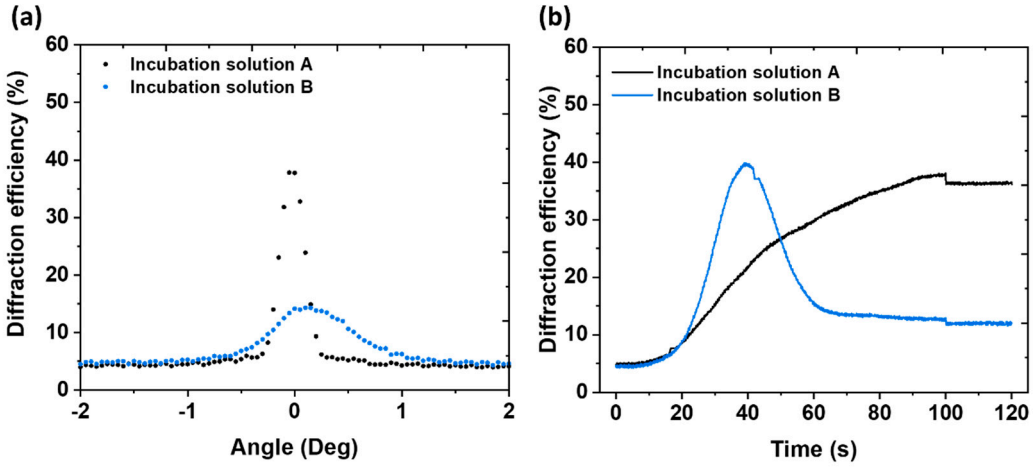

Figure 3. (a) Variation of the DE during the recording process, the real-time growth of DE in (AM/PA) hydrogel incubated with incubation solution A and B can be observed and, (b) variation of the DE with the incidence angle (Bragg curves) of the recorded VTGs.

To achieve better final DE, VTG were recorded again with incubation solution B, but the laser exposure of the sample was stopped by the shutter when the diffraction efficiency started to decrease (Figure S2a). As expected, higher DE was obtained when the exposition time was decreased (Figure

Preprints (www.preprints.org) | NOT PEER-REVIEWED | Posted: 31 July 2023 doi:10.20944/preprints202307.2074.v1

S2b). Diffraction efficiency of VTG measured after the recording, in the Bragg curve, where the DE was recorded varying the incidence angle, was higher than that observed in real time during the recording processed. The decrease in diffraction efficiency observed in real-time (Figure 3) is most probably associated to the shrinkage of the hydrogel VTG that occurred during recording. In addition, an increased scattering of the diffraction produced by VTGs recorded with incubation solution B was observed. This behaviour is due to the high concentration of monomer and crosslinker, which leads to the formation of a much harder and crosslinked VTG with a slight white colour due to the increased scattering. However, it worth noting that this effect was not observed in the layers incubated with solution A. Thus, it was decided to use incubation solution A, as maintaining the same recording parameters used with solution B resulted in holographic gratings with a higher diffraction efficiency. Furthermore, it was possible to record VTGs of different dimensions: first, spots of 1.45 cm^2 were recorded, and later, considering their further expansion in water, smaller spots of 0.84 cm^2 were recorded (Figure 4). This parameter is important in view to use the holograms for biosensing. For example, for the functionalisation with the DNA receptor, less probe material will be required while for the complete functionalization of the VTG area.

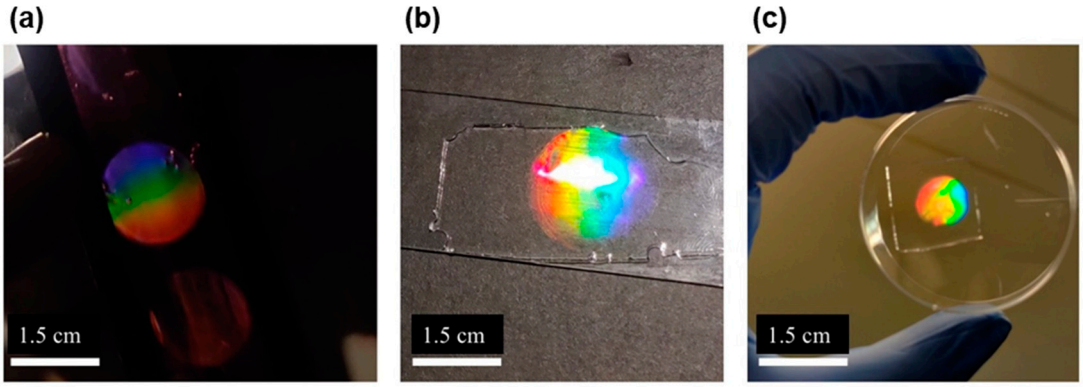

Figure 4. Digital photos of the transmission phase volume gratings recorded in (AM/PA) hydrogel layers: recorded spots of (a) 1.45 cm^2 after recording and (b) 2.72 cm^2 after first wash with distilled water; (c) smaller recorded spots of 0.84 cm^2 which (image not shown), after the first washing with distilled water, reached a size of 1.56 cm^2.

Further, using real-time monitoring of the recording process, different incubation times were tested with incubation solution A: 1, 2 and 3 days of incubation. DE was real-time monitored and Bragg curves were obtained after the recording (Figure 5, Table 3). The hydrogel layers were exposed for up to 100 s for holographic recording; it was observed that, after exposure, the diffraction efficiency continues to be stable. As it can be seen from the results, the dynamic linear range increases with increasing incubation days from 1 to 2, obtaining a DE of 80% in the later. Interestingly, the curve of hydrogels incubated for 3 days showed a significant inhibition time, the hydrogel layers incubated for 3 days start recording the transmission gratings after 40 seconds of laser light exposure, whereas the hydrogels incubated for 1 and 2 days show a faster response by starting the recording process within the first 20 seconds of exposure and at 100 s the DE was 50% for hydrogels incubated for 3 days, which is lower than that obtained at 2 days. The behaviour of the real-time diffraction efficiency is associated with the diffusion of the incubation solution within the hydrogel, which gradually decreases over time as the hydrogel layer begins to dry out. Probably, 2 days of incubation, allowed the complete absorption of the incubation solution and an optimal and reproducible holographic recording with high diffraction efficiency.

Preprints (www.preprints.org) | NOT PEER-REVIEWED | Posted: 31 July 2023 doi:10.20944/preprints202307.2074.v1

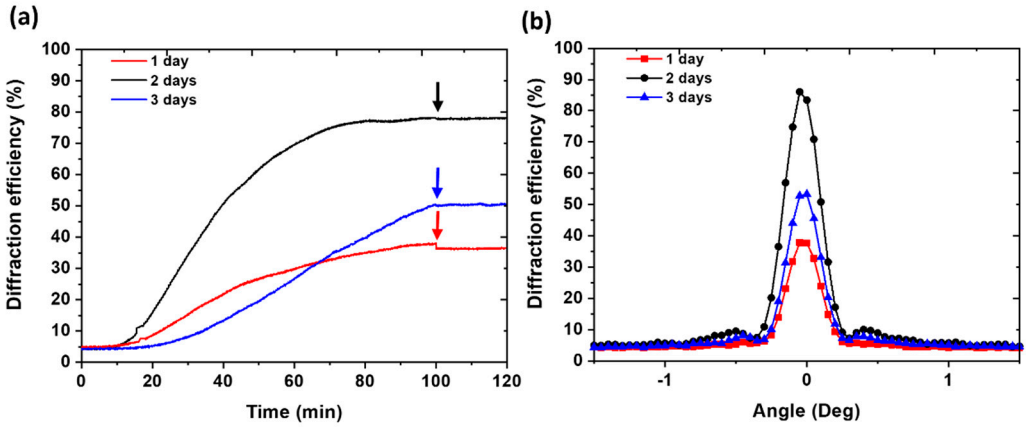

Figure 5. Real-time growth curve of DE% and the corresponding Bragg curves after 1, 2 and 3 days of incubation with incubation solution A.

Table 3. Characterisation of unslanted volume grating obtained after delivering 200 µL of incubation solution and evaluating different incubation times.

Incubation time (days)	Layer thickness (µm)	Recording beams intensity (mW/cm²)	Recording exposure time (s)	Maximum DE achieved (%)
1	300	7.5	100	40
2	300	7.5	100	80
3	300	7.5	100	50

To study the VTG hydrogel stability, Bragg selectivity curves were measured just after recording of hydrogels incubated for 1 day with incubation solution A and after multiple overnight washing step with distilled water (Figure 6). After the first washing step, the components that did not react during the formation of the volume transmission gratings are washed away, which is reflected in a slight change in diffraction efficiency around 10%.

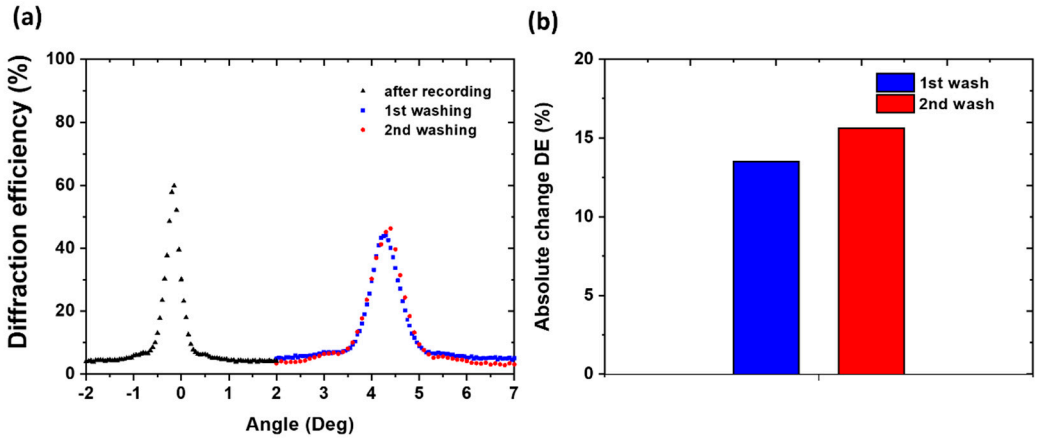

Figure 6. (a) Bragg selectivity curves of (AM/PA) hydrogel layers obtained after recording with 60 % DE and after two overnight washes with approximately 44-46 % DE. (b) Histogram of absolute DE% change after washing steps.

The observed broadening of the Bragg selectivity curve after the washing step can be explained by the dimensional change of the layer due to the swelling of the hydrogel grating. Thus, the recorded

Preprints (www.preprints.org) | NOT PEER-REVIEWED | Posted: 31 July 2023 doi:10.20944/preprints202307.2074.v1

hydrogel grating swells and expands, resulting in a slight increase in fringe spacing. Although hydrogels are generally soft and elastic, the stable and interconnected 3D crosslinked structure of the optimized hydrogel (AM/PA) allowed for stable volumetric diffractive structures.

To obtain the thickness and refractive index modulation of the recorded gratings, Bragg's angular selectivity curves were fitted using Kogelnik's coupled-wave theory [25]. An initial simulation was performed on a VTG with 35% diffraction efficiency (Figure S3, Supporting Information). Then, the theoretical fitting was performed on the Bragg curve obtained under the optimized conditions 80% DE (Figure S4, Supporting Information). Both Bragg curves obtained from the simulation are in good agreement with the respective experimental curves. The simulation results are summarized in Table 4.

Table 4. Results obtained by fitting Bragg selectivity curves.

	VTG thickness (μm)	Refractive index modulation (RIM)
after recording	190	0.0010
1st washing	60	0.0015
2nd washing	62	0.0017

Furthermore, the Bragg curve of the optimized volume gratings was characterized over time to test how the diffraction efficiency and/or the fringe spacing are affected when the hydrogel starts to dry (Figure 7). In this experiment, the Bragg curves of the (AM/PA) hydrogel layers were obtained at controlled times and temperature and relative humidity conditions were also monitored. The fringe spacing (Λ) was calculated with the Equation (2):

$$\Lambda = \frac{\lambda}{2\sin\left[\frac{(\text{peak } \theta_1 - \text{peak } \theta_2)}{2}\right]} \quad (2)$$

Where λ is the wavelength of the probe beam and (peak θ_1 – peak θ_2) is the angle calculated in the Bragg curve between the two Bragg peaks. From the results, it was possible to observe a gradual decrease in diffraction efficiency already after one hour of sample drying at RT, while the fringe spacing did not change significantly during time. It can be observed that even when the hydrogel is dry, about 30% of the initial DE% is retained. At the same time, it can also be seen that the change in VTG period as the hydrogel dries over time is almost negligible (about 1%).

Preprints (www.preprints.org) | NOT PEER-REVIEWED | Posted: 31 July 2023 doi:10.20944/preprints202307.2074.v1

(a)

Time (min)	DE (%)
30	64.98
60	58.31
120	38.36
180	31.38
240	19.40

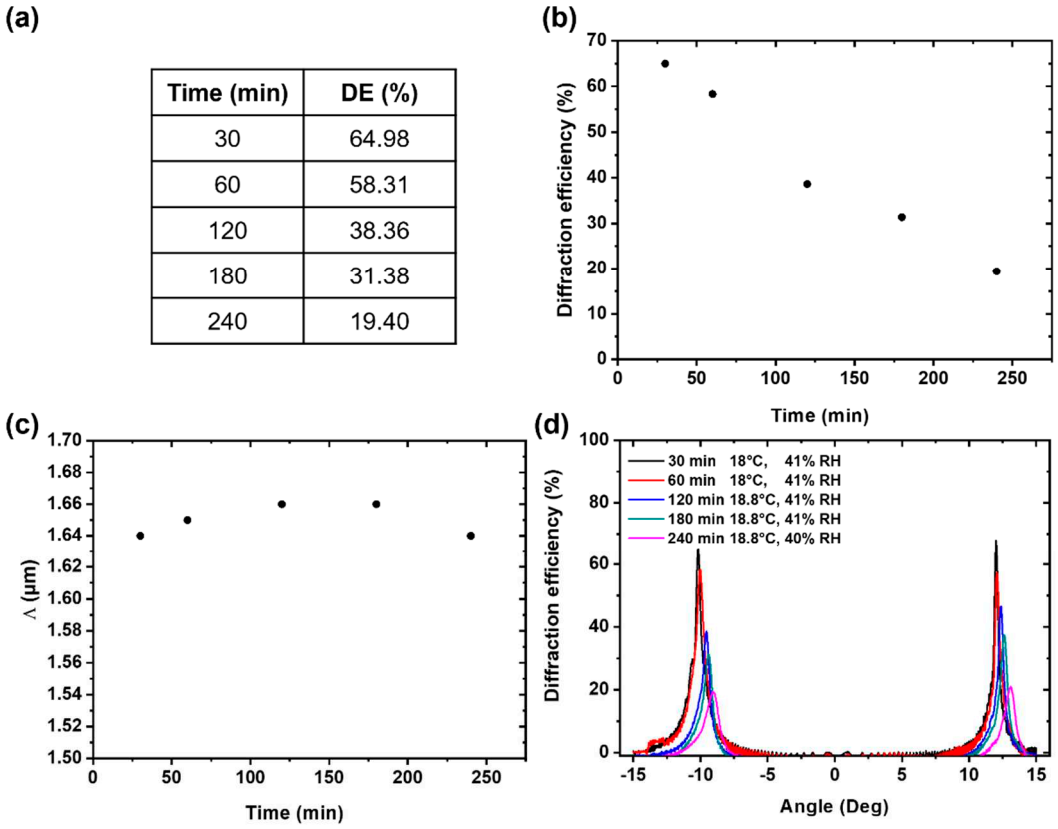

Figure 7. (a) Data of the hydration state study and (b) Diffraction efficiency change over time; (c) Bragg selectivity curves of (AM/PA) hydrogel layer while drying over time and (d) fringe spacing versus time.

Biofunctionalization of VTGs and Hybridization assays by fluorescence detection

Some of the hydrogels recorded with volume gratings were subjected to analysis of hybridization ability with complementary strands using fluorescence detection. For that, starting from a VTG with a DE of 20% in water, they were conditioned in SSC1x, and diffraction diminished to one half. Then, VTG conditioned in SSC1x were incubated with a solution 5 μM of an oligonucleotide probe bearing a thiol group in THF:Ac-TCEP 1:1, and irradiated for 30 minutes, according to the protocol described for biofuncionalization [23]. After washing with SSC1x for several hours, the diffraction efficiency decreased by 40%.

Then, the VTG hydrogel was submitted to serial incubations with increasing concentrations of Cy5-labeled oligonucleotides (0.2; 0.5; 1 and 2 μM) having the complementary sequence of the immobilized probe for 1 h, each condition was assayed by triplicate. After each incubation, the VTG was washed with SSC1x for 1 h, and the fluorescence was recorded. The same experiment was carried out with a biofunctionalized VTG but using a non-complementary sequence for the hybridization, as a control of the specificity in the target biorecognition.

As it can be observed in Figure 8, the fluorescence increased with the concentration of complementary strand while in the case of hybridization with non-complementary target only residual fluorescence remained inside the VTG hydrogel. Thus, it was concluded that the probe was successfully immobilized inside the VTG keeping its bioavailability to hybridize in a specific manner. Furthermore, VTG hybridized with the complementary target keeps their diffractive capacity (Figure S5, Supporting Information).

Preprints (www.preprints.org) | NOT PEER-REVIEWED | Posted: 31 July 2023 doi:10.20944/preprints202307.2074.v1

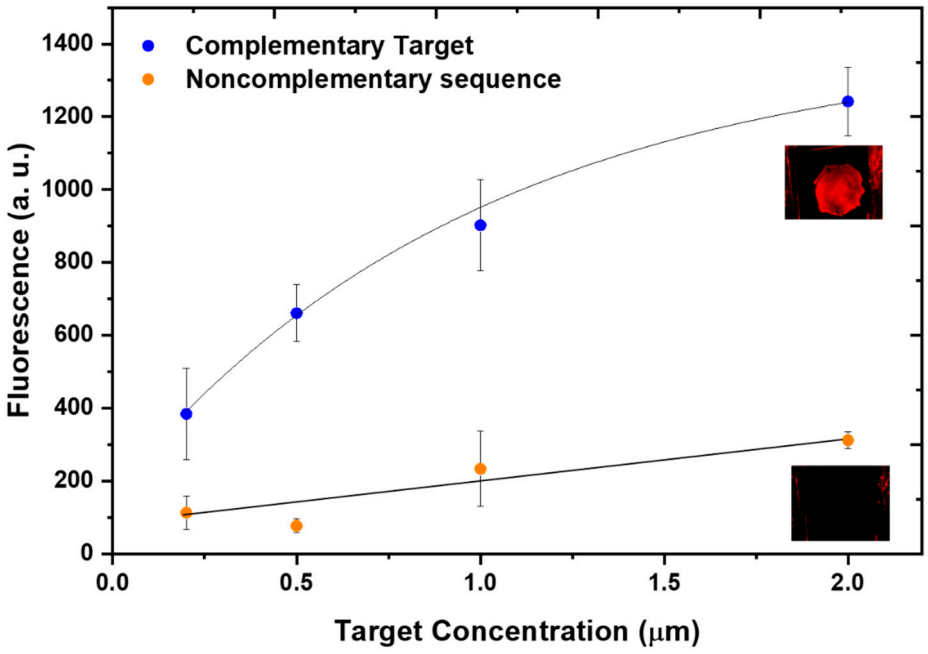

Figure 8. Fluorescence intensity of VTG hydrogels biofunctionalized with an oligonucleotide probe and incubated with increasing concentrations of labeled complementary target (blue) or labeled non-complementary sequence (orange) washed with SSC1x for 1h.

Then, to characterize the prepared hydrogels, and to demonstrate their robustness, the reusability of the biofunctionalized hydrogels was tested. For that a biofuncionalized VTG hybridized with the complementary labeled oligonucleotide was subjected to different dehybridization conditions and the dehybridization was monitored by fluorescence (Figure 9a). As expected, the initial fluorescence (target incubation) decreased considerably after SSC1x washing. Then, it slightly decreased after dehybridization with water washing, and even more when temperature was applied, however, a residual fluorescence still remained inside the VTG hydrogel. That indicated that the hydrogel was not fully dehybridized. The complete dehybridization was achieved when 50% formamide in SSC1x was used, as in this case, fluorescence signal disappeared totally. The VTG hydrogel, fully dehybridized, was submitted to another hybridization cycle, and the corresponding control, with a non-complementary target was also done. Figure 9b shows the fluorescence signal after washing with SSC1x. After the dehybridization, specific hybridization was again achieved, demonstrating the reusability of the bioresponsive hydrogel. Although typically one-shot assay is used in biosensing protocols, the reusability test gives a characterization of the material robustness.

 doi:10.20944/preprints202307.2074.v1

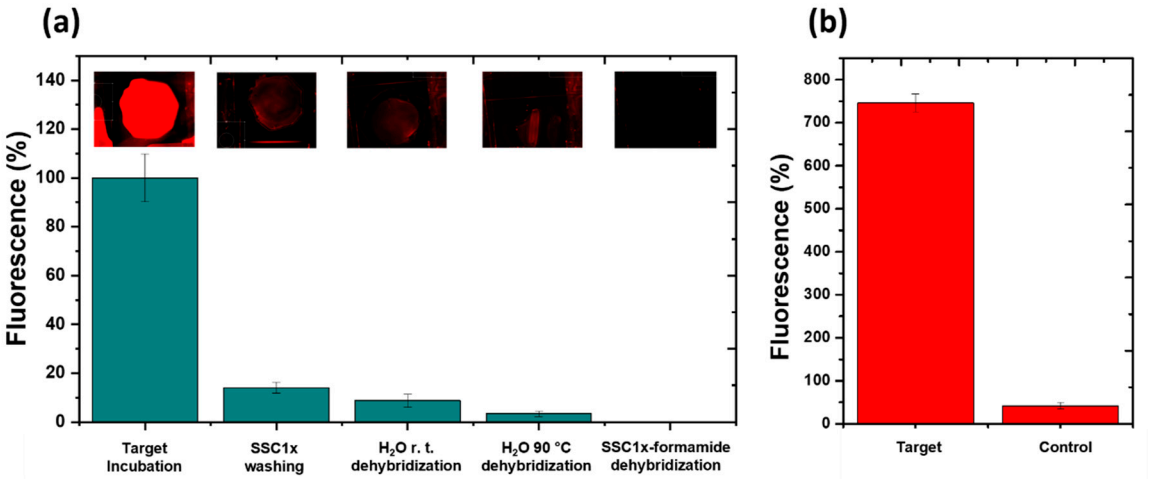

Figure 9. a) Fluorescence (%) measured after target hybridization, washing with SSC1x, and after the several dehybridization conditions. All the fluorescence images were capture using the same acquisition conditions (gain and exposition time). Fluorescence was normalized to the maximum signal (target incubation). b) Fluorescence of the VTG hydrogel dehybridized with SSC1Cx-formamide after a second cycle of hybridization with a complementary target and a non-complementary target control labeled with cy5. Incubation was carried out for 1h in SSC1x and washing was performed for 1h in SSC1x.

4. Conclusions

Unslanted volume transmission gratings (VTGs) were recorded in an Acrylamide/Propargyl acrylate hydrogel layer with good reproducibility and good optical quality. The conditions of the incubation and recording processes were successfully optimized and VTG hydrogels were optically characterized. Furthermore, the volume hydrogel gratings were found to be stable in water, maintaining their diffraction efficiency even after successive washes. The holographic recording optimisation process performed in hydrogel layers can be useful for the design of potential holographic biosensors. The hydrogel VTGs can be biofunctionalized with an oligonucleotide probe, being able to act as a bioresponsive material, hybridizing only with the complementary strand target, and keeping their diffractive capacity. The reusability of the bioresponsive hydrogel for several hybridization cycles has been also demonstrated. Thus, these three-dimensional hydrogel networks with embedded diffractive structures are promising candidates for analysis of targets involved in diseases and health monitoring.

Supplementary Materials: The following supporting information can be downloaded at the website of this paper posted on Preprints.org.

Author Contributions: Conceptualization, P.Z., I.N., M.I.L. and M.-J.B., methodology, P.Z., I.N., M.I.L. and M.-J.B., formal analysis, P.Z., I.N., M.I.L. and M.-J.B., investigation, M.I.L, M.-J.B., P.Z. and I.N.; writing original draft preparation, M.I.L, M.-J.B., P.Z. and I.N.; writing review and editing, P.Z., I.N., M.I.L. and M.-J.B., Á.M., supervision, I.N., Á.M. and M.-J.B.; funding acquisition, I.N., Á.M. and M.-J.B. All authors have read and agreed to the published version of the manuscript.

Funding: This work was financially supported by the E.U. FEDER, the Spanish Ministry of Science and Innovation (ADBIHOL-PID2019-110713RB-I00/AEI/10.13039/501100011033) and Generalitat Valenciana (PROMETEO/2020/094). M. I. Lucío acknowledges MINECO for her Juan de la Cierva-Incorporación grants (IJC 2018-035355-I). P. Zezza acknowledges the Generalitat Valenciana for her S. Grisolia grant and the UPV for the mobility grant (BEFPI 2022). Funded with Aid for First Research Projects (PAID-06-22), Vice-rectorate for Research of the Universitat Politècnica de València (UPV).

Institutional Review Board Statement: Not applicable.

Informed Consent Statement: Not applicable.

Data Availability Statement: Not applicable.

Conflicts of Interest: The authors declare no conflict of interest.

References

1. Yetisen, A.K.; Naydenova, I.; Da Cruz Vasconcellos, F.; Blyth, J.; Lowe, C.R. Holographic Sensors: Three-Dimensional Analyte-Sensitive Nanostructures and Their Applications. *Chem. Rev.* **2014**, *114*, 10654–10696, doi:10.1021/cr500116a.
2. Blanche, P.A. Holographic Recording Media and Devices. *Encycl. Mod. Opt.* **2018**, *1–5*, 87–101, doi:10.1016/B978-0-12-803581-8.09610-7.
3. Mihaylova, E.M. Water-Soluble Holographic Photopolymers for a Sustainable Future—A Review. *Coatings* **2022**, *12*, 1765, doi:10.3390/coatings12111765.
4. Pal, A.K.; Labella, E.; Goddard, N.J.; Gupta, R. Photofunctionalizable Hydrogel for Fabricating Volume Optical Diffractive Sensors. *Macromol. Chem. Phys.* **2019**, *220*, 1–8, doi:10.1002/macp.201900228.
5. Sun, X.; Agate, S.; Salem, K.S.; Lucia, L.; Pal, L. Hydrogel-Based Sensor Networks: Compositions, Properties, and Applications - A Review. *ACS Appl. Bio Mater.* **2021**, *4*, 140–162, doi:10.1021/acsabm.0c01011.
6. Madduma-Bandarage, U.S.K.; Madihally, S. V. Synthetic Hydrogels: Synthesis, Novel Trends, and Applications. *J. Appl. Polym. Sci.* **2021**, *138*, 1–23, doi:10.1002/app.50376.
7. Fouassier, J.P.; Allonas, X.; Burget, D. Photopolymerization Reactions under Visible Lights: Principle, Mechanisms and Examples of Applications. *Prog. Org. Coatings* **2003**, *47*, 16–36, doi:10.1016/S0300-9440(03)00011-0.
8. Mikulchyk, T.; Martin, S.; Naydenova, I. Humidity and Temperature Effect on Properties of Transmission Gratings Recorded in PVA/AA-Based Photopolymer Layers. *J. Opt.* **2013**, *15*, 105301 doi:10.1088/2040-8978/15/10/105301.
9. Toal, V. Photopolymers: Beyond the Standard Approach to Photosensitisation. *J. Eur. Opt. Soc. - Rapid Publ.* **2009**, *4*, 1–4, doi:10.2971/jeos.2009.09042.
10. Ramírez, M. G.; Lucío, M. I.; Morales-Vidal, M.; Beléndez, A.; Bañusl, M.-J.; Maquieira, Á., Pascual, I. Holographic Transmission Gratings Stored in a Hydrogel Matrix. *Photosensit. Mater. their Appl.* **2020**, *SPIE 11367*. 113670B. doi: 10.1117/12.2555362
11. Berramdane, K.; Ramírez, M.G.; Zezza, P.; Lucío, M.I.; Bañuls, M.J.; Maquieira, Á.; Morales-Vidal, M.; Beléndez, A.; Pascual, I. Processing of Holographic Hydrogels in Liquid Media: A Study by High-Performance Liquid Chromatography and Diffraction Efficiency. *Polymers.* **2022**, *14*, 2089. doi:10.3390/polym14102089.
12. Naydenova, I.; Jallapuram, R.; Howard, R.; Martin, S.; Toal, V. Investigation of the Diffusion Processes in a Self-Processing Acrylamide-Based Photopolymer System. *Appl. Opt.* **2004**, *43*, 2900–2905, doi:10.1364/AO.43.002900.
13. Gleeson, M.R.; Sheridan, J.T. A Review of the Modelling of Free-Radical Photopolymerization in the Formation of Holographic Gratings. *J. Opt. A Pure Appl. Opt.* **2009**, *11*, doi:10.1088/1464-4258/11/2/024008.
14. Davies, S.; Hu, Y.; Jiang, N.; Blyth, J.; Kaminska, M.; Liu, Y.; Yetisen, A.K. Holographic Sensors in Biotechnology. *Adv. Funct. Mater.* **2021**, *31*, doi:10.1002/adfm.202105645.
15. Lucío, M.I.; Cubells-Gómez, A.; Maquieira, Á.; Bañuls, M.J. Hydrogel-Based Holographic Sensors and Biosensors: Past, Present, and Future. *Anal. Bioanal. Chem.* **2022**, *414*, 993–1014, doi:10.1007/s00216-021-03746-1.
16. Marshall, A.J.; Young, D.S.; Blyth, J.; Kabilan, S.; Lowe, C.R. Metabolite-Sensitive Holographic Biosensors. *Anal. Chem.* **2004**, *76*, 1518–1523, doi:10.1021/ac030357w.
17. Mikulchyk, T.; Walshe, J.; Cody, D.; Martin, S.; Naydenova, I. Humidity and Temperature Induced Changes in the Diffraction Efficiency and the Bragg Angle of Slanted Photopolymer-Based Holographic Gratings. *Sensors Actuators, B Chem.* **2017**, *239*, 776–785, doi:10.1016/j.snb.2016.08.052.
18. Irfan, M.; Martin, S.; Naydenova, I. Temperature-Sensitive Holograms with Switchable Memory. *Adv. Photonics Res.* **2021**, *2*, 2100062, doi:10.1002/adpr.202100062.
19. Bianco, G.; Ferrara, M.A.; Borbone, F.; Zuppardi, F.; Roviello, A.; Striano, V.; Coppola, G. Volume Holographic Gratings as Optical Sensor for Heavy Metal in Bathing Waters. *Opt. Sensors 2015* **2015**, *9506*, 95062B, doi:10.1117/12.2179171.
20. Yetisen, A.K.; Qasim, M.M.; Nosheen, S.; Wilkinson, T.D.; Lowe, C.R. Pulsed Laser Writing of Holographic Nanosensors. *J. Mater. Chem. C* **2014**, *2*, 3569–3576, doi:10.1039/c3tc32507e.
21. Elsherif, M.; Hassan, M.U.; Yetisen, A.K.; Butt, H. Wearable Contact Lens Biosensors for Continuous Glucose Monitoring Using Smartphones. *ACS Nano* **2018**, *12*, 5452–5462, doi:10.1021/acsnano.8b00829.
22. Davies, S.; Hu, Y.; Blyth, J.; Jiang, N.; Yetisen, A.K. Reusable Dual-Photopolymerized Holographic Glucose Sensors. *Adv. Funct. Mater.* **2023**, *33*, doi:10.1002/adfm.202214197.
23. Zezza, P.; Lucío, M. I.; Fernández, E.; Maquieira, Á.; Bañuls, M.-J. Surface Micro-Patterned Biofunctionalized Hydrogel for Direct Nucleic Acid Hybridization Detection. **2023**, 13, 312, doi:10.3390/bios13030312.

24. Naydenova, I. *Holographic Sensors*; Elsevier Inc., **2019**; ISBN 9780128154670.
25. Kogelnik, H. Coupled Wave Theory for Thick Hologram Gratings. *Bell Syst. Tech. J.* **1969**, *48(9)*, 2909–47.
26. Mira, D.; Llorente, R.; Morais, S.; Puchades, R.; Maquieira, A.; Marti, J. High-Throughput Screening of Surface-Enhanced Fluorescence on Industrial Standard Digital Recording Media. *Opt. Based Biol. Chem. Sens. Def.* **2004**, *5617*, 364, doi:10.1117/12.578301.